RESEARCH REPOSITORY

This is the author's final version of the work, as accepted for publication following peer review but without the publisher's layout or pagination. The definitive version is available at:

Wiśniewski, M., Koter, S., Terzyk, A.P., Włoch, J. and Kowalczyk, P. (2017) CO 2 - reinforced nanoporous carbon potential energy field during CO 2 /CH 4 mixture adsorption. A comprehensive volumetric, in-situ IR, and thermodynamic insight. Carbon.
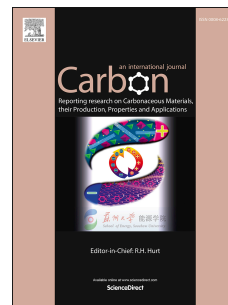
http://researchrepository.murdoch.edu.au/id/eprint/37567/

Accepted Manuscript

CO$_2$ - reinforced nanoporous carbon potential energy field during CO$_2$/CH$_4$ mixture adsorption. A comprehensive volumetric, *in-situ* IR, and thermodynamic insight

Marek Wiśniewski, Stanisław Koter, Artur P. Terzyk, Jerzy Włoch, Piotr Kowalczyk

CO_2 - reinforced nanoporous carbon potential energy field during CO_2/CH_4 mixture adsorption. A comprehensive volumetric, *in-situ* IR, and thermodynamic insight

Marek Wiśniewski[1,2], Stanisław Koter[3], Artur P. Terzyk[1,*], Jerzy Włoch[4],

Piotr Kowalczyk[5]

[1] Faculty of Chemistry, Physicochemistry of Carbon Materials Research Group, Nicolaus Copernicus University in Toruń, Gagarin Street 7, 87-100 Toruń, Poland

[2] INVEST-TECH R&D Center, Plaska Street 32-34, 87-100 Toruń, Poland

[3] Faculty of Chemistry, Department of Physical Chemistry, Nicolaus Copernicus University in Toruń, Gagarin Street 7, 87-100 Toruń, Poland

[4] Faculty of Chemistry, Synthesis and Modification of Carbon Materials Research Group, Nicolaus Copernicus University in Toruń, Gagarin Street 7, 87-100 Toruń, Poland

[5] School of Engineering and Information Technology, Murdoch University, Murdoch 6150 WA, Australia

(*)Corresponding author: Artur P. Terzyk

Tel: (+48) (56) 611-43-71, E-mail: aterzyk@chem.umk.pl

Abstract: CO_2/CH_4 mixture adsorption is very important in different fields like, for example, a biogas purification. Using a comprehensive experimental approach based on volumetric and *in-situ* FTIR measurements the new results of CO_2/CH_4 mixture separation on a carbon film are reported. The application of this experimental approach makes it possible to elaborate the effect of enhanced CH_4 adsorption at low CO_2 concentrations in the adsorbed phase. The presence of this effect is proved experimentally for the first time. This effect is responsible for the deviation of Ideal Adsorption Solution model from the experimental data. To discuss separation mechanism the activity coefficients at constant spreading pressure values are calculated. At low spreading pressure, CO_2 activity coefficient is strongly disturbed by the presence of CH_4 molecules in the surface mixture. In contrast, the CH_4 activity coefficients are remarkably influenced by adsorbed CO_2 only at higher CO_2 surface concentrations. The

1

obtained activity coefficients are successfully described by a new modification of the Redlich-Kister equation. This modification takes into account the interaction between binary mixture components and an adsorbent. Finally we show that the studied carbon possesses very good CO_2/CH_4 mixture separation properties, comparable to those reported for other adsorbents.

Keywords: adsorption, activated carbon, CO_2/CH_4 mixture, FTIR, thermodynamics, IAS.

1. Introduction

CO_2/CH_4 mixture has been considered as very important because it is a major biogas component [1] produced by bacteria from anaerobic fermentation of a biodegradable waste. A biogas is currently one of the most important renewable energy sources. However, before a biogas is used, CO_2 should be removed [2] since this component lowers the gas heating value. Among more or less advanced procedures of a biogas purification, adsorption-based methods (for example the Pressure Swing Adsorption [3]) play an important role, and activated carbons (and carbonaceous materials) are still considered as the most promising adsorbents [4]. This is caused by energy-efficiency and cost effectiveness of the adsorption-based methods and generally, by a relatively low cost of activated carbons. However, the major difficulty with activated carbons application is relatively low selectivity to CO_2 [5], thus the experimental as well as simulation studies of CO_2/CH_4 mixture have been reported, to optimize properties of the "best possible" carbon material. Among carbon materials, studied in the molecular simulations of CO_2/CH_4 mixture adsorption, one can mention a model carbon slit-like micropores, triply periodic carbon minimal surfaces, and Virtual Porous Carbons (VPC) [6].

Mentioned above theoretical studies are important not only in the field of a biogas purification, but simulations have shed a new light on the mechanism of the so-called "enhanced coal bed methane recovery process". This process is important in the reduction of anthropogenic CO_2. Considering CO_2/CH_4 mixture adsorption, a two-stage mechanism of the process has been reported, and the influence of pore sizes and surface oxidation on this mechanism has been studied theoretically. It is suggested that in very narrow micropores and at low mixture pressures, adsorbed CO_2 molecules can enlarge the potential field in pores, and drag some methane molecules from the gas phase. In this way, CH_4 adsorption (*via* dispersive interactions) can be increased in micropores [7]. This effect can be caused by the permanent

quadrupole moment of CO_2 molecule, and in general, by larger tendency of CO_2 to intermolecular interactions. Thus, adsorbed CO_2 molecules can induce permanent electric moments in adsorbed CH_4 molecules. However, at larger CO_2 pore concentrations, the dominant CO_2-CO_2 interactions can lead to the displacement of CH_4 molecules from small pores. It is interesting that similar effect was reported for some Metal Organic Framework (MOF) materials. It was shown that water preadsorption should increase adsorption of CO_2 [8]. Summing up, molecular simulations suggest the occurrence of this enhancement effect at low pressures, however, (up to our knowledge) the experimental data confirming this effect do not exist.

Using adsorption measurements reinforced by the *in-situ* Fourier Transform Infra Red (FTIR) spectroscopy results, we are able to get deeper insight into the mechanism of CO_2/CH_4 mixture adsorption and separation. Special attention has been paid to the enhancement of CH_4 storage due to preadsorbed CO_2 (as it is described above). By the application of adsorption thermodynamics we discuss the mechanism of adsorption and separation in narrow carbon micropores. Unexpected plots of CO_2 activity coefficients are reported. It is shown that in narrow carbon nanopores the interaction between the adsorbent, CO_2 and CH_4 is more complicated as it has been proposed till now. Finally we show that studied nanoporous carbon is a potential candidate for CO_2/CH_4 mixture separation, and that the IAS based separation coefficients should be treated with a care.

2. Experimental methods

A carbon film used in this study was prepared from a pure cellulose. The charring experiments were described in detail elsewhere [9-11]. The cellulose film heated at 573 K in air for 1 h was outgassed at 873 K for 1 h under the dynamic vacuum (1.3 10^{-6} bar) to remove surface oxygen. The full structural characteristics of the tested adsorbent have been described previously [12]. Briefly, based on the results of low-temperature Ar and N_2 adsorption, the tested carbon film can be regarded as a strictly microporous solid with the BET surface area equal to 478.3 m^2/g (carbon labeled C_{873} in [12]). It is important that the pore size distribution (calculated using the Density Functional Theory method) shows mainly the presence of very narrow micropores with the diameter equal to 0.62 nm (and the volume equal to 0.19 cm^3/g). Our previous simulation studies showed [6] that the most effective carbon for CO_2/CH_4

mixture separation should possess pores with diameters smaller than c.a. 1 nm, thus the studied carbon is a perfect candidate for this purpose.

The *in-situ* FTIR studies were carried out in a vacuum cell described previously [9,10, 13]. The application of this technique makes it possible to determine in what extent physical or chemical adsorption occurs. Moreover, we can easily determine the absence of any surface oxygen compounds formed by chemisorption. We can also, based on the spectra of carbon, check in what extent a carbon material changes its structure during adsorption and in what extent a sample is affected by possible impurities.

The construction of the *in-situ* FTIR cell enables the thermal treatment of the carbon film up to 1200 K in any controlled atmosphere or in a vacuum. The CO_2 and CH_4 adsorption was performed under isothermal conditions (T = 298 K). For each run (see Tab.1) after adsorption of CH_4, the CO_2 partial pressure was changed by addition of the next portion of the gas. The spectra for the samples were recorded using the Mattson Genesis II FTIR spectrophotometer. Spectral changes accompanying adsorption of gases were used, after calibration, to describe quantitatively observed phenomena. The respective gas phase was a background for each carbon film spectrum, enabling the observation of spectral changes of a sample surface, without perturbation from the gas phase. A period of at least 5 h (monitoring continuously) at each gas composition was held in order to be sure that the equilibrium was achieved.

Additionally, the adsorption isotherms of separate gases were measured volumetrically (T = 298 K).

All experiments were repeated at least three times and qualitatively similar results were obtained. The presented results are representative for three tested series of experiments.

Table 1. The parameters of experimental runs; p is the sum of pCH_4 and pCO_2 at the end of experiment, yCO_2 is the equilibrium mole fraction of CO_2 in the gas phase.

Run number	pCH_4 [bar]	p [bar]	yCO_2
1	0.065	0.20	0.68
2	0.13	0.40	0.67
3	0.20	0.47	0.58
4	0.26	0.53	0.52
5	0.34	0.67	0.49
6	0.41	0.78	0.48

4

Fig.1 shows the FTIR spectra obtained after exposing the studied carbon sample to CH_4/CO_2 gas mixture at increasing partial CO_2 pressure. To the best of our knowledge there is a lack of *in-situ* FTIR studies using carbonaceous materials as molecular sieves in the CO_2/CH_4 separation process. What is important, adsorption of the gas mixture on carbon surface does not cause the appearance of any oxygen-containing surface compounds, particularly carbonate or carbonyl groups. It means that adsorption of both compounds is physical and fully reversible.
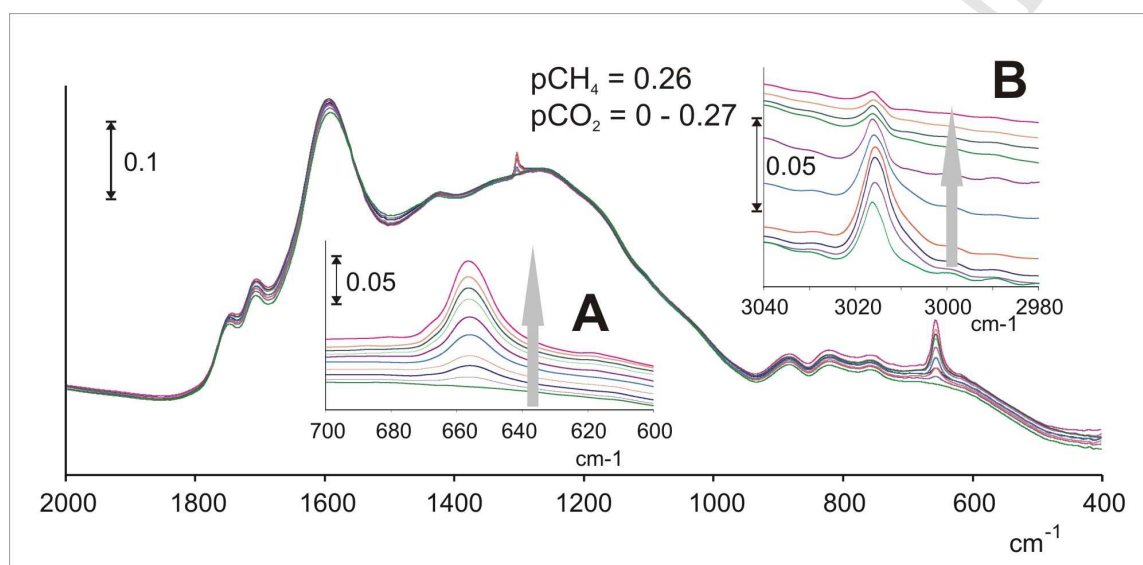
Figure 1. The FTIR spectra of studied carbon film recorded after exposure to CH_4/CO_2 gas-mixture ($pCH_4 = 0.26$ bar, $pCO_2 = 0$-0.27 bar) at 298 K. Insets: the CO_2 bending region (A); and CH stretching region (B).

At 298 K the increase in the CO_2 pressure causes first the increase, and then the decrease in the intensities of the bands observed for physically adsorbed CH_4 (at 3016 cm^{-1}). The occurrence of this maximum during physical adsorption of CH_4 stays in an excellent agreement with the results of previous theoretical reports [7], and is the major subject of this work.

3. Results and discussion

The experimental adsorption data for pure gases are shown in Fig.2. As in the case of "ordinary" microporous activated carbons, the adsorption of CO_2 is larger than the adsorption

5

of CH_4 (see for example [15-17]). This is mainly caused by larger potential energy of $C-CO_2$ interactions in very narrow micropores [7]. This also causes that the equilibrium CO_2/CH_4 selectivity at "zero" coverage is enhanced in very narrow micropores.

As it has been often proposed [18], adsorption data were fitted using the Dubinin and Astakhov (DA) [19] adsorption isotherm equation (Fig.2). Both studied gases are supercritical at the measurement temperature, therefore the "pseudo saturated vapour pressure" should be calculated. To do this the method proposed by Amankwah and Schwarz (AS) [20] was applied. As it was shown recently [18] application of the AS approach leads to the best fit of the DA model to simulated CO_2 and CH_4 adsorption isotherms [18]. As it is seen from Fig.2 the DA model fits our experimental data very well (Fig.2). The determination coefficient (showing the fit of DA model to experimental data) is higher than 0.9999. The values of k (a parameter of the AS equation [20]) were across the range of 2.1-2.7 (i.e. typical values for microporous carbons [20]). In the case of gas mixtures, because of the irregular shape of curves, a Spline function (interpolation order = 2) was used to fit the experimental data (see Fig.3).
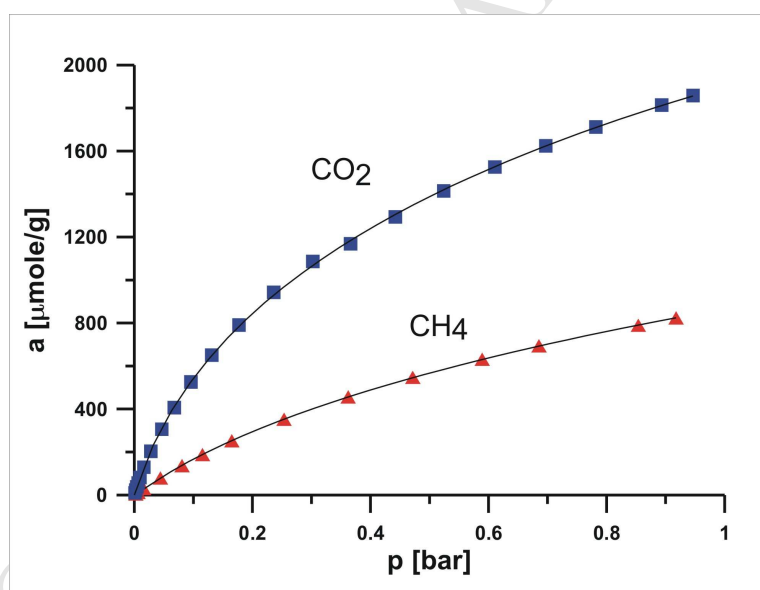
Figure 2. Experimental data of pure gas adsorption at T = 298 K (points) and their fitting by the DA equation (lines) with the AS "pseudo saturated vapour pressure".

Fig.3 shows the experimental data of mixture adsorption. Considering the data collected in Fig.3A one can conclude that the effect of enhanced CH_4 adsorption occurs especially at larger CH_4 pressures. What is interesting, with increasing CH_4 pressure the maximum methane adsorption occurs at lower yCO_2 (Fig.3C). In Figs.3A-D, the prediction of

gas adsorption according to the Ideal Adsorbed Solution (IAS) theory is also shown ($a_i = x_i a$). The total adsorption of gases, $a = a_1 + a_2$, was calculated from [14]:

$$a = \left(x_1 / a_1^o + x_2 / a_2^o \right)^{-1} \qquad (1)$$

where the mole fraction of i-th adsorbate, x_i, is obtained from eqs. (2b), (4) and (5) (here $\gamma_i = 1$). It is seen that the IAS theory cannot predict the presence of maxima observed for CH_4 (Figs.3A and 3D). It is obvious because the maxima are caused by interactions between the mixture components. For the CO_2 adsorption the discrepancy between the experiment and the IAS theory is not so large, especially at low partial pressure of CH_4 (Fig.3B). However, with the rise in pressure, (and with the rise in yCO_2 - see Fig.3D) the deviations between theory and experiment become larger.
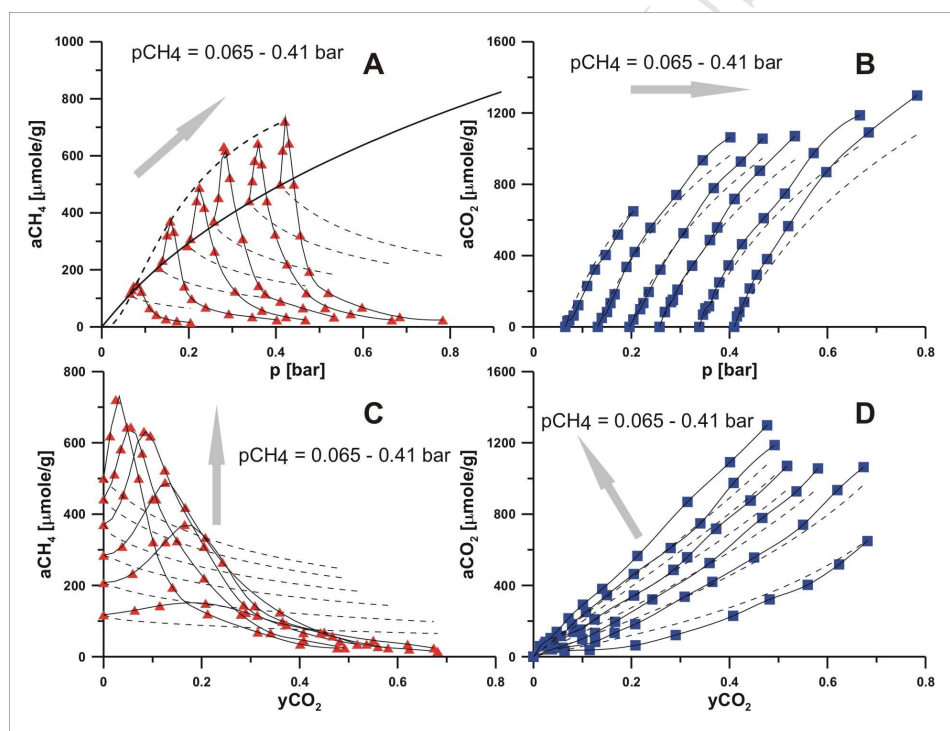
Figure 3. (A) and (B): adsorption of CH_4 and CO_2 vs. total pressure p.(C) and (D): adsorption of CH_4 and CO_2 vs. yCO_2; at each run pCH_4 = const.; the arrows show runs 1-6 (Tab.1). Solid lines - the interpolation (a Spline function with interpolation order = 2), dashed line - the IAS theory. Bold solid and dashed lines in figure (A) show the isotherm for pure CH_4 and the approximation of $aCH_{4\ max}$ by the DA adsorption isotherm equation, respectively.

The height of the peaks, aCH$_{4\ max}$, observed on aCH$_4 = f(p)$ and aCH$_4 = f(y$CO$_2)$ increases with p (Fig.3A) and with pCH$_4$ (Fig.3C). As one can see (Fig. 3A - bold dotted line), aCH$_{4\ max} = f(p)$ can be described using the DA adsorption isotherm equation. Thus, in the studied range of pressures the effect of enhanced CH$_4$ adsorption becomes stronger with the mixture pressure, as well as with the pressure of methane in the mixture. Moreover, from the data collected in Fig.4 one can conclude that yCH$_{4\ max}$ slightly increases with pCH$_4$. This dependence is of sigmoidal form. The lower limit of yCH$_{4\ max}$ ($p \rightarrow 0$) seems to be ca. 0.81, the upper limit is 1. Thus, increasing the methane pressure in the mixture leads to increase in the methane gas mole ratio at with maximum methane adsorption occurs.
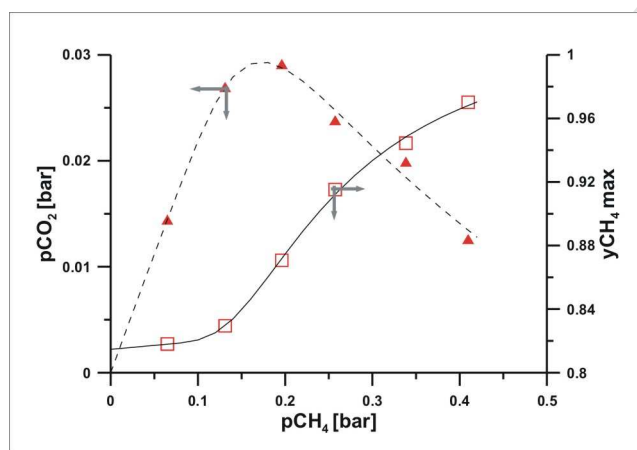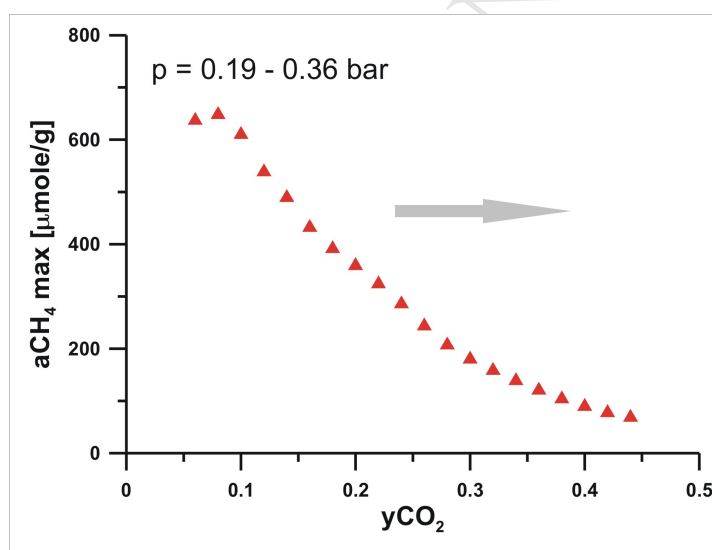

Figure 4. The relation between yCH$_{4\ max}$ and pCH$_4$ (solid line shows a sigmoidal fitting) and the dependence between pCO$_2$ and pCH$_4$ at aCH$_{4\ max}$.

The relation between pCO$_2$ and pCH$_4$, at which aCH$_{4\ \textbf{max}}$ is observed, is also shown in Fig.4. As one can observe pCO$_2$ reaches a maximum at pCH$_4$ = ca. 0.18 bar. As pCO$_2$ is related to pCH$_4$ by pCO$_2 = p$CH$_4(1-y$CH$_4)/y$CH$_4$, the observed maximum is caused by the fact that yCH$_{4\ max}$ increases with pCH$_4$ (see ashed line in Fig.4).

The adsorption data $a_i = f(p)$, i = CH$_4$, CO$_2$, at yCO$_2$ = const., obtained from $a_i(p)$ (shown in Fig.3) are presented in Fig.5 (p is restricted to the experimental range). These dependences are needed to calculate the activity coefficients. Here also the maximum of aCH$_4$ is observed. The maxima for yCO$_2 \leq 0.04$ are not visible because of too low pressure. The maximum decreases with the rise in yCO$_2$ (Fig.6).

8
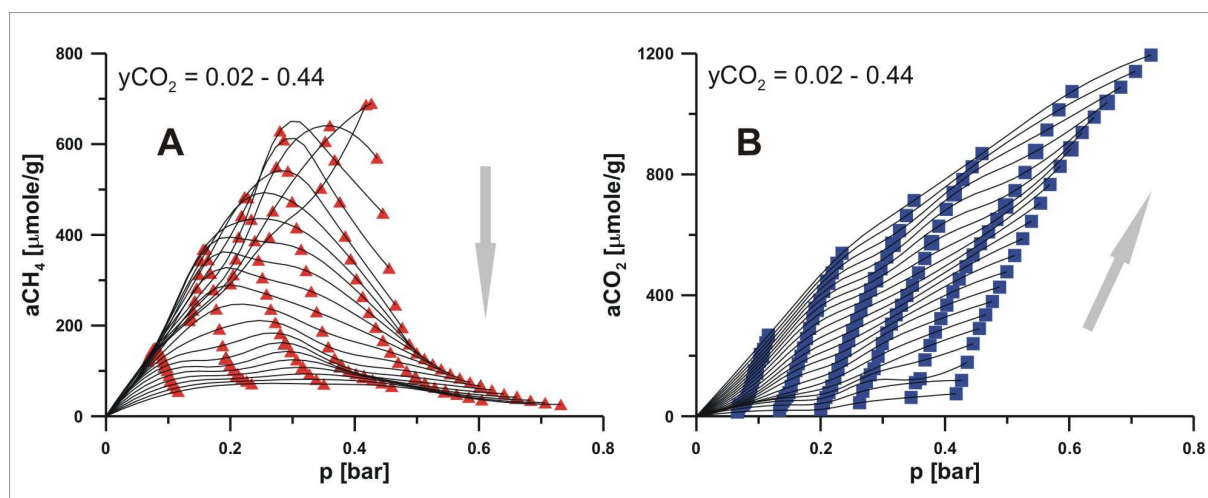
Figure 5. The plots of $a_i = f(p)$, i = CH$_4$, (A) CO$_2$, (B) at yCO$_2$ = const., yCO$_2$ across the range of 0.02-0.44, with the step = 0.02; symbols indicate points calculated from the spline interpolation of the experimental data shown in Figs. 3A, B, lines present interpolation of these points using a Spline function.

Figure 6. The relation between yCO$_2$ and the maxima, aCH$_4$ max, on the curves aCH$_4$= $f(p)$ at yCO$_2$ = const. (Fig.5); here total pressure changes nonmonotonically from 0.19 up to 0.36 bar.

In Fig.7 aCO$_2$ is plotted vs. p (at pCO$_2$ = const.). It is seen that the influence of methane pressure (pCH$_4$) on carbon dioxide adsorption (aCO$_2$) is practically negligible.
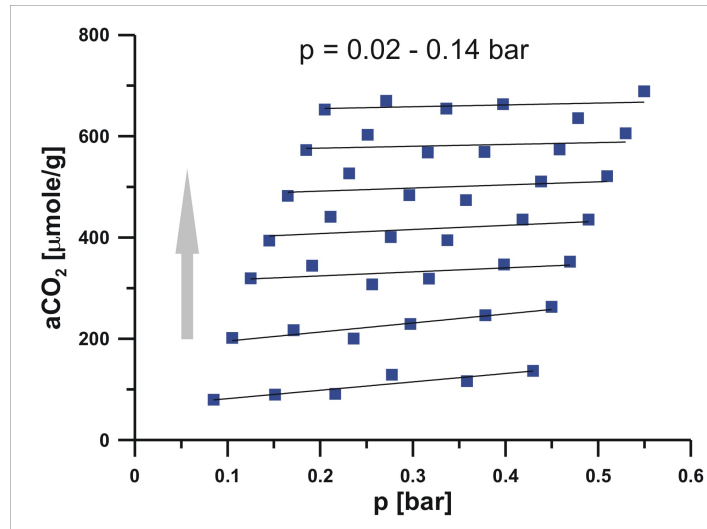
Figure 7. The plots of $aCO_2 = f(p)$ (at $pCO_2 = $ const.), pCO_2 across the range of 0.02 - 0.14 with the step 0.02; $p = pCO_2 + pCH_4$; solid line - the linear regression.

To get a deeper insight into the mechanism of CO_2/CH_4 mixture separation the activity coefficients of adsorbed molecules were calculated according to Myers and Prausnitz [14], using the equalities:

$$\pi = \pi_1^o = \pi_2^o \tag{2a,b}$$

where π, π^o_i is the spreading pressure for the gas mixture, and for a pure gas adsorption, respectively. To calculate π from:

$$\pi^* = \frac{A}{RT}\pi = \int_0^p \frac{a_1 + a_2}{p} dp \ , \ y_i = \text{const.} \tag{3}$$

a_1 and a_2 were fitted as a function of p for different values of y_1, and π^o_i is given by [14]:

$$\pi_i^{o*} = \frac{A}{RT}\pi_i^o = \int_0^{p_i^o} \frac{a_i^o}{p} dp \qquad i = 1, 2 \tag{4}$$

where A is the specific surface area of an adsorbent, a_i - the number of moles of adsorbed i-th component per unit mass of an adsorbent, R, T are the gas constant and the absolute

10

temperature, p_i^o, a_i^o are the pressure and adsorption of a pure *i-th* gas, respectively. From the equality of the chemical potentials of the adsorbate in the gas phase and in the adsorbate solution, we can relate p_i^o corresponding to π by [14]:

$$p_i^o(\pi) = p_i / \gamma_i x_i = y_i p / \gamma_i x_i \qquad (5)$$

where x_i and γ_i are the mole fraction and the activity coefficient of the *i*-th component in the adsorbed solution, respectively, p_i is the partial pressure of i in the gas mixture ($p_i = y_i p$). Basing on our experimental conditions, we assume that the studied gas mixture behaves ideally. The activity coefficients γ_1 and γ_2 were obtained from eqs. (1a,b,5) and x_i determined experimentally.

Figs.8A and 8B collect the experimental adsorption values at $\pi^* =$ const. One can observe the progressive displacement of CH_4 by CO_2. Some maxima at low xCO_2 (occurring at small π^* values) are caused by the enhanced CH_4 adsorption by adsorbed CO_2 molecules (see Fig.8B). The activity coefficients are plotted in Figs.8C and 8D as the function of xCO_2 (at $\pi^* =$ const.). It is seen that γCH_4 very slightly depends on π^* and the dependence $\gamma CH_4 = f(xCO_2)$ is "typical" [21] it is going to 1 for $xCO_2 \rightarrow 0$ and increases with xCO_2. In contrast, γCO_2 strongly depends on π^*. It shows maxima at lower, and minima at high values of π^*, respectively. At $\pi^* =$ ca. 800 μmol/g γCO_2 it is close to 1.

The results of recent GCMC study of CO_2/CH_4 adsorption on a series of VPC models [21] are very helpful for the analysis of the activity coefficients plots collected in Fig.8. Namely, similar plot of the CH_4 activity coefficients were observed for the simulated CH_4 adsorption data (see Fig. 10 in [21]). Thus, taking into account the plot of γCH_4 one can conclude, that during the progressive displacement of CH_4 by CO_2 from micropores of the studied carbon, reinforced by CO_2 carbon force field causes only small deviation of γCH_4 from ideality (see the inset in Fig.8D). However, if the amount of adsorbed CO_2 becomes larger γCH_4 drastically increases.
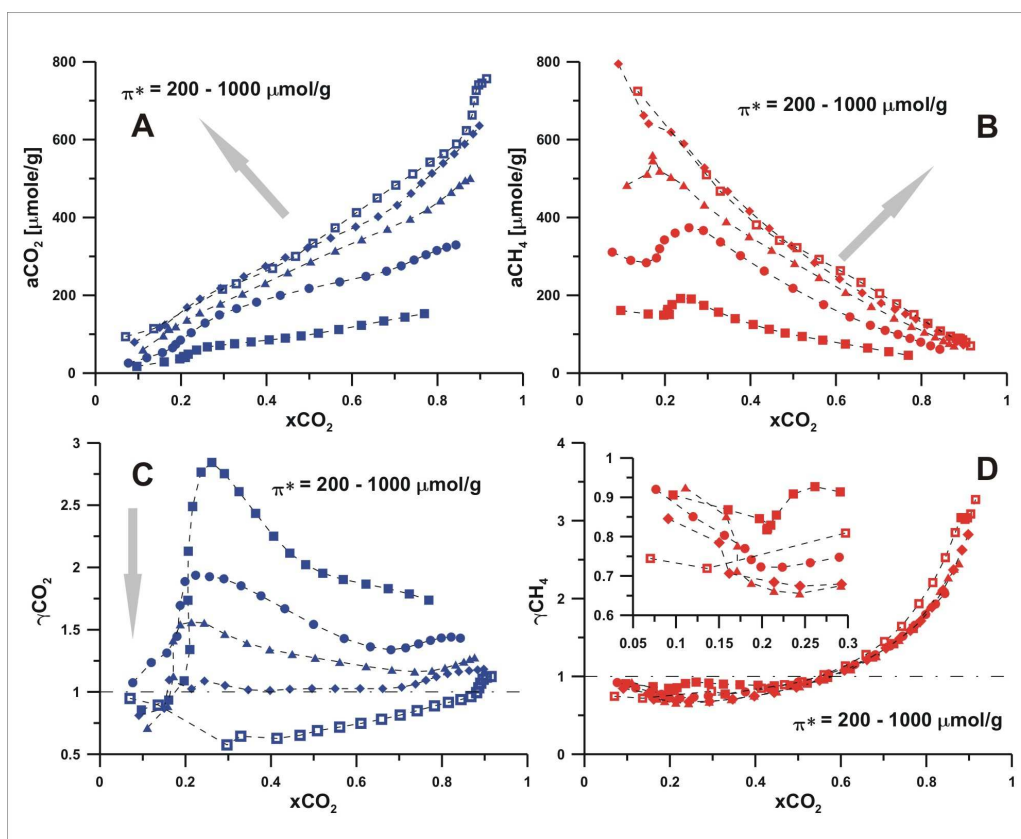
Figure 8. (A) and (B): $a_i = f(xCO_2)$. (C) and (D): $\gamma_i = f(xCO_2)$; for $\pi^* = 200, 400, 600, 800$ and 1000 µmol/g.

On the other hand, the influence of CH_4 molecules on the behaviour of γCO_2 is drastic, especially in the range of low π^* values. Although we observe that CO_2 molecules enlarge the potential field in micropores and drag some methane molecules from the gas phase (as it was suggested by previous GCMC simulation data [7]) the behaviour of γCO_2 observed during experiment (Fig.8C) is different than it was predicted by the simulation [21]. Thus, up to our knowledge, the existing binary mixture models (for example proposed by Siperstein and Myers [22], Redlich and Kister [23] and others [24]) are unable to describe CO_2 and CH_4 activity coefficients reported in Fig.8C and 8D. This leads to the conclusion that in very narrow real carbon micropores the C-CO_2-CH_4 interactions are more complex than presumed.

One of the possible methods taking into account the complex nature of the studied system is the application of a new expansion describing the molar excess of Gibbs free enthalpy (G^{ex}). The modification of the Redlich-Kister equation [23] taking into account the interaction between binary mixture components and an adsorbent can be written as [21]:

12

$$\frac{G^{ex}}{RT} = x_1 x_2 (A_{12} + B_{12}(x_1 - x_2)) + x_1 x_3 (A_{13} + B_{13}(x_1 - x_3)) + x_2 x_3 (A_{23} + B_{23}(x_2 - x_3)) \qquad (6)$$

where: A_{ik} and B_{ik} are the parameters of expansion related to the interactions between components i and k (note that $k=3$ denotes an adsorbent). After simple manipulation this leads to the activity coefficients given by [21]:

$$\ln \gamma_1 = -x_1 x_2 (A_{12} - 2B_{12}(1 + x_2 - x_1)) - x_1 x_3 (A_{13} - 2B_{13}(1 + x_3 - x_1)) + x_2 (A_{12} - x_2 B_{12})$$
$$+ x_3 (A_{13} - x_3 B_{13}) - x_2 x_3 (A_{23} + 2B_{23}(x_2 - x_3)) \qquad (7)$$

$$\ln \gamma_2 = -x_1 x_2 (A_{12} - 2B_{12}(1 + x_2 - x_1)) - x_2 x_3 (A_{23} - 2B_{23}(1 + x_3 - x_2)) + x_1 (A_{12} + x_1 B_{12})$$
$$+ x_3 (A_{23} - x_3 B_{23}) - x_1 x_3 (A_{13} + 2B_{13}(x_1 - x_3)) \qquad (8)$$

As previously [21], x_3 can be expressed as:

$$x_3 = 1 - (a_1 + a_2) / a_{max} \qquad (9)$$

whereas x_1 and x_2 are replaced by x_i for the binary mixture:

$$x_i(bin) = a_i / (a_1 + a_2) \qquad (10)$$

using the relation:

$$x_i(bin) = x_i(bin)(1 + x_3), i = 1, 2 \qquad (11)$$

Before the eqs.(6)-(11) were applied to description of the activity coefficients collected in Figs.8C and 8D, some model numerical calculations were performed. We tried to check how the exclusion of arbitrarily chosen parameter (and/or the set of parameters) can change the quality of the fit to experimental data. The obtained results confirm that the exclusion of the parameters responsible for the interaction of gas mixture components with studied carbon surface drastically reduce the fit quality.

The arbitrarily chosen results of fitting are collected in Figs.9A-C and in Supplementary data (Figs.S1). As one can see, the quality of the fit is quite good. We observe the linear dependence of eqs.(6-8) parameters on π^* (Figs.S2A-S2C).
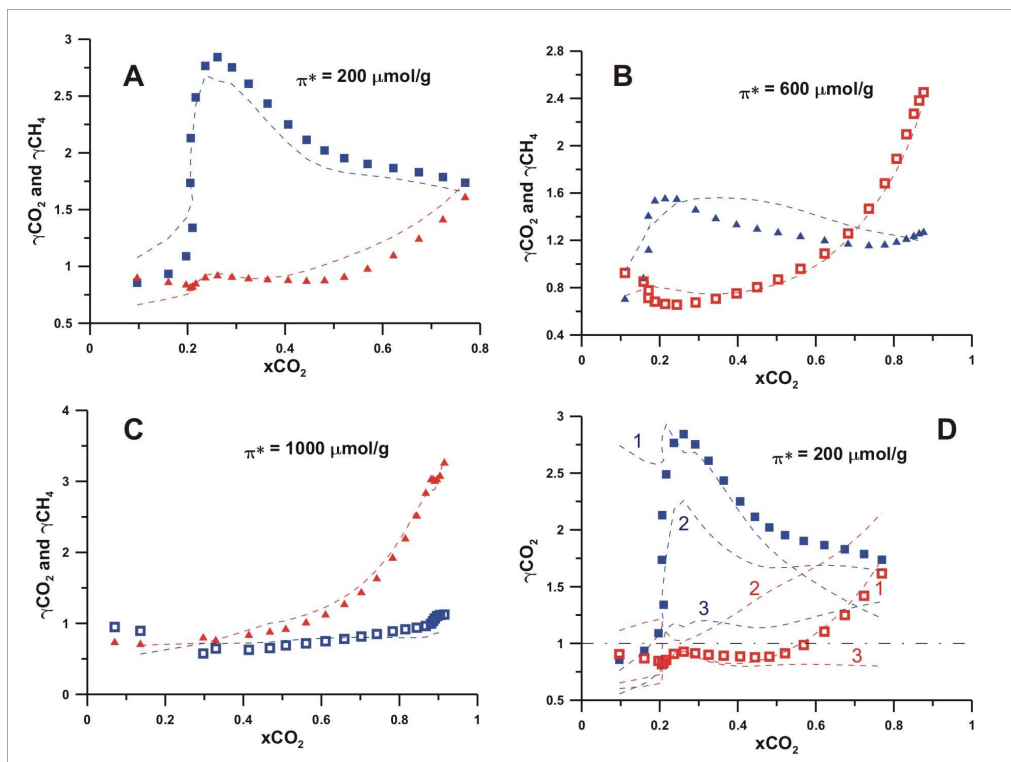

Figure 9. The fit of theoretical CO_2 (blue dashed lines) and CH_4 (red dashed lines) activity coefficients to experimental data (blue and red symbols for CO_2 and CH_4, respectively) for π^* = 200 (A), 600 (B) and 1000 (C) $\mu mol/g$. (D): the changes in the values of γCO_2 (blue dashed lines) and γCH_4 (red dashed lines) for A_{13} and $B_{13} = 0$ (1), A_{23} and $B_{23} = 0$ (2), and A_{12} and $B_{12} = 0$ (3) (π^*=200 $\mu mol/g$).

In Fig.9D we also show how γCO_2 and γCH_4 depend on the values of interaction parameters. One can observe that A_{13} and B_{13} as well A_{12} and B_{12} values are responsible for the appearance of a characteristic maximum on the γCO_2 plot observed at low π^* values. From Figs.S2A-C one can also conclude that the B_{23} parameter only slightly depends on π^*. To get more information about the energetics of adsorption, as well as about the physical meaning of the parameters the values of free enthalpy of mixing (ΔG^{mix}) were calculated using procedure proposed by Myers and Prausnitz [14]. The results collected in Fig.10A show very important properties of the studied system. First of all one can observe the rise in absolute ΔG^{mix} value

14

with the rise in π^*. It means that for increasing amount of CO_2 in the mixture the process becomes more spontaneous. This is caused by the polarity of adsorbed molecules, i.e. larger potential energy of lateral CO_2-CO_2 than CO_2-CH_4 interactions (the critical temperature of CO_2 is equal to 304 K, while for CH_4 it is equal to 190.9 K). Moreover, for low π^* values,
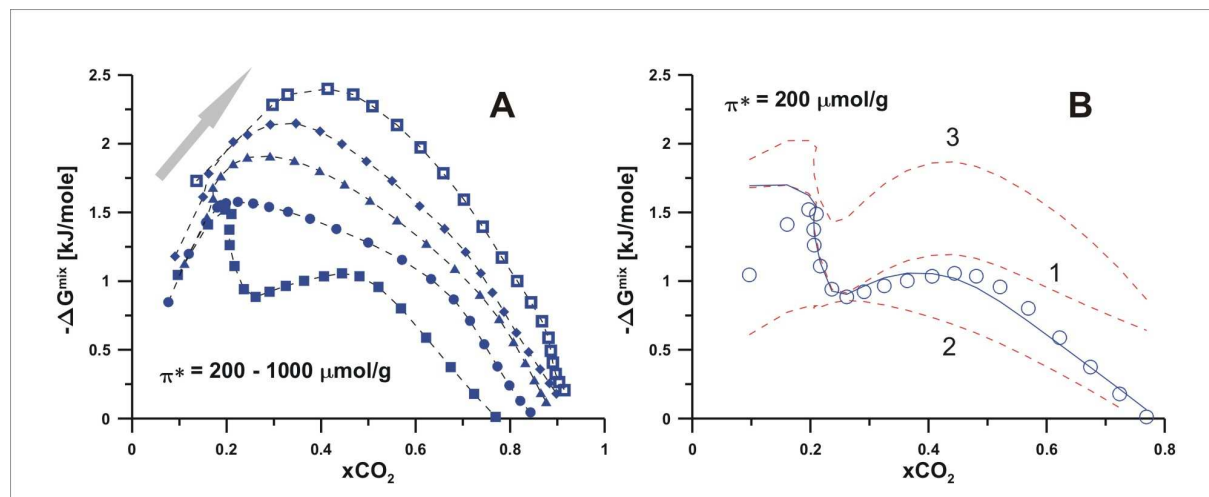
Figure 10. (A) Excess free enthalpy of mixing. Gray arrow shows the rise in π^*. (B) The plots of this enthalpy calculated for the data from Fig.9D for A_{13} and $B_{13} = 0$ (1), A_{23} and $B_{23} = 0$ (2), and A_{12} and $B_{12} = 0$ (3) (π^*=200 µmol/g). Circles show the plot of ΔG^{mix} for $\pi^* = 200$ µmole/g, solid line shows the fit to experimental data.

one can see two specific maxima on ΔG^{mix} plots. The first one is due to the effect of enhanced CH_4 adsorption, the second one is resulted mainly by CO_2-CO_2 interactions in micropores. However, at larger π^* values, with increasing CO_2 contribution in the adsorbed mixture, the both maxima overlay.

On the other hand, the results of ΔG^{mix} calculations (Fig.10B) have shed a new light on the meaning of the parameters of eqs.(6-8). One can see that A_{13} and B_{13} (curve 1) are responsible for ΔG^{mix} at the limit of large xCO$_2$ values. Next pair of the parameters (A_{23} and B_{23}, respectively - curve 2) is responsible for the (mentioned above) maxima on ΔG^{mix} plots, reflecting fluid-fluid intermolecular interactions in the adsorbed phase. Finally, the data collected on Fig.10B (curve 3) show that A_{12} and B_{12} parameters are mainly responsible for the placing the ΔG^{mix} plot on the energy scale. However, further studies of other experimental systems are necessary to elucidate the meaning of the discussed parameters in details.

3.2. Separation coefficients

15

To check the separation properties of an adsorbent one can calculate the experimental separation coefficient S defined by:

$$S(CO_2/CH_4) = \frac{xCO_2/xCH_4}{yCO_2/yCH_4} \tag{12}$$

The respective plots are collected in Fig.11.
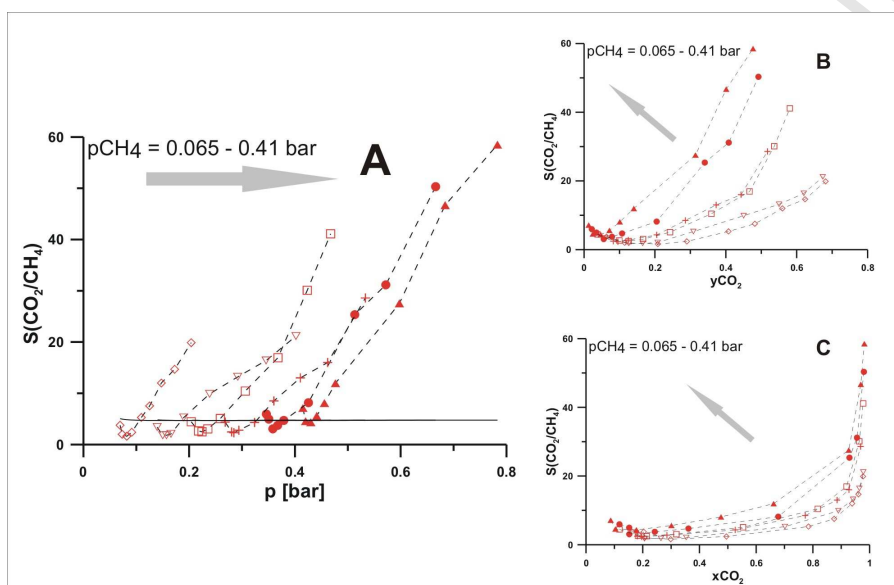
Figure 11. The separation coefficients of CO_2 over CH_4 (eq.(12)) plotted as the function of p, (A, solid lines - the IAS predictions), yCO_2 (B) and xCO_2 (C).

As it was mentioned in the Introduction the problem of CO_2/CH_4 mixture separation is very important, and the number of papers devoted to this problem is enormous. In Tab.2 we collect selected results published in 2017 for different adsorbents (at T close to used in our study). One can observe that the $S(CO_2/CH_4)$ values are usually calculated by the application of the IAS theory. Fig.10A shows that for our systems the IAS-based separation coefficients are practically pressure independent. This is not in agreement with the experimental results (Fig.11). The results from Tab.2, together with the data plotted in Fig.11 lead to the conclusion about very high CO_2/CH_4 selectivity of the studied carbon film. One can observe the small decrease in S at low p, yCO_2 and xCO_2 is induced by the (reported in this study) effect of enhanced CH_4 adsorption by CO_2.

16

Table 2. Selected results of $S(CO_2/CH_4)$ for different adsorbents (data reported in 2017).

Reference number	Adsorbent	p [bar]	$S(CO_2/CH_4)$
[25]	MIL- 53(Cr) and MIL- 53(Cr)/ graphene oxide composites	up to 4	2-12[*]
[26]	Carbonyl-incorporated aromatic polymers	up to 1	6.6-23
[27]	Cd(II) MOF	up to 1	22-18.4[*]
[28]	Co-polyimides containing bis [4-(4-aminophenoxy) phenyl] sulfone	4	47.2-51.9
[29]	Different nanoporous materials	1.2	2.0-256.4
[30]	C-xx and EC-xx polymers	1	2.6-3.4[*]
[31]	Zn(II)/Cd(II) MOF	1	5.2-6[*]
[32]	Microporous silicalite -1	1	4.7-5.7[*]
[16]	Activated carbon from wood pellets	up to 20	2-8[*]
[33]	MIL-100 (Fe)	up to 30	10-30[*]
[34]	Sulfur-doped nanoporous carbons	1	5-23[*]
This study	Cellulose based carbon	up to 1	1.8-58.5, (4.7-5) [*]

(*) calculated using the IAS theory

4. Conclusions

The results of a comprehensive experimental approach used for the CO_2/CH_4 mixture adsorption/separation study on a microporous activated carbon film are reported. The *in-situ* FTIR, applied for the study of this system for the first time, is a major used technique.

Obtained adsorption data for pure gases are very well described by the DA isotherm equation with the AS "pseudo saturated vapour pressure" approach. The effect of enhanced CH_4 adsorption by CO_2 molecules is observed experimentally for the first time. CH_4 maximum adsorption increases with the pressure, and it is also well predicted by the DA

model. CH_4 mole fraction at the maximum adsorption increases with the CH_4 partial pressure and varies in the range 0.8 - 1 depending on that pressure. The enhanced by CO_2 methane adsorption leads to inapplicability of the IAS model. Our data analysis shows that CO_2 has a very strong influence on CH_4 adsorption. In contrast, CH_4 molecules practically do not change the CO_2 adsorption. Obtained activity coefficients of CH_4 slightly decrease in the range of enhanced CH_4 adsorption however, the drastic changes in γCH_4 are observed if the mole fraction of CO_2 in adsorbate exceeds ca. 0.7. In contrast, CO_2 activity coefficients are strongly influenced by CH_4 molecules, especially in the range of low spreading pressures ($\pi^* \leq 600$ μmol/g) and in the area of enhanced CH_4 adsorption.

Obtained experimental activity coefficients can be successfully described by the proposed recently [21] modification of the Redlich-Kister equation [23] taking into account the interaction between binary mixture components and an adsorbent. Obtained parameters of this modified equation linearly depend on π^*. The plots of excess free enthalpy of mixing make it possible to perform the analysis of the energetics of the process. Also the meaning of the Redlich-Kister equation parameters has been expalined.

Finally it is shown that the studied carbon possess very good CO_2/CH_4 mixture separation properties, comparable to those reported recently in the literature for other adsorbents. Obtained IAS-based separation coefficients are pressure independent, and this is not in agreement with the experimental data reported in this study. Because the separation coefficients are usually calculated based on the IAS theory, they should be treated with a care especially for the case of adsorption in carbons possessing very narrow nanopores.

Appendix A. Supplementary data.

References

[1] J.L. Pinilla, S. de Llobet, I. Suelves, R. Utrilla, M.J. Lázaro, R. Moliner, Catalytic decomposition of methane and methane/CO_2 mixtures to produce synthesis gas and nanostructured carbonaceous material, Fuel 90 (2011) 2245-2253.

[2] F. Wang, S. Fu, G. Guo, Z.Z. Jia, S.J. Luo, R.B. Guo, Experimental study on hydrate-based CO_2 removal from CH_4/CO_2 mixture, Energy 104 (2016) 76-84.

[3] Y.J. Kim, Y.S. Nam, Y.T. Kang, Study on a numerical model and PSA (pressure swing adsorption) process experiment for CH_4/CO_2 separation from biogas, Energy 91 (2015) 732-741.

[4] M. Kacem, M. Pellerano, A. Delebarre, Pressure swing adsorption for CO_2/N_2 and CO_2/CH_4 separation: Comparison between activated carbons and zeolites performances, Fuel Proces. Technol. 138 (2015) 271 -283.

[5] L. Pino, C. Italiano, A. Vita, C. Fabiano, V. Recupero, Sorbents with high efficiency for CO_2 capture based on amines-supported carbon for biogas upgrading, J. Environm. Sci. 48 (2016) 138-150.

[6] S. Furmaniak, P. Kowalczyk, A.P. Terzyk, P.A. Gauden, P.J.F. Harris, Synergetic effect of carbon nanopore size and surface oxidation on CO_2 capture from CO_2/CH_4 mixtures, J. Coll. Interf. Sci. 397 (2013) 144-153.

[7] P. Kowalczyk, P.A. Gauden, A.P. Terzyk, S. Furmaniak, P.J.F. Harris, Displacement of methane by coadsorbed carbon dioxide is facilitated in narrow carbon nanopores, J. Phys. Chem. C 116 (2012) 13641-13649.

[8] A.O. Yazaydin, A.I. Benin, S.A. Faheem, P. Jakubczak, J.J. Low, R.R. Willis, et al. Enhanced CO_2 adsorption in metal-organic frameworks via occupation of open-metal sites by coordinated water molecules, Chem. Mater. 21 (2009) 1425-1430.

[9] J. Zawadzki, M. Wiśniewski, An infrared study of the behavior of SO_2 and NO_x over carbon and carbon-supported catalysts, Catal. Today 119 (2007) 213-218.

[10] M. Wiśniewski, Mechanistic aspects of N_2O decomposition over carbon films and carbon-film-supported catalysts. Catal. Lett. 144 (2014) 633-638.

[11] J. Zawadzki, M. Wiśniewski, Adsorption and decomposition of NO on carbon and carbon-supported catalysts. Carbon 40 (2002) 119-124.

[12] A.P. Terzyk, P.A. Gauden, J. Zawadzki, G. Rychlicki, M. Wiśniewski, P. Kowalczyk, Toward the characterisation of microporosity of carbonaceous films. J. Coll. Interf. Sci. 243 (2001) 183-192.

[13] J. Zawadzki, Infrared spectroscopy in surface chemistry of carbons. Chem. Phys. Carbon 21 (1989) 147-380.

[14] A.L. Myers, J.M. Prausnitz, Thermodynamics of mixed-gas adsorption, AIChE J. 11 (1965) 121-127.

[15] M. Rungta, G.B. Wenz, C. Zhang, L. Xu, W. Qiu, J.S. Adams, et al. Carbon molecular sieve structure development and membrane performance relationships, Carbon 115 (2017) 237-248.

[16] J.F. Vivo-Vilches, A.F. Pérez-Cadenas, F.J. Maldonado-Hódar, F. Carrasco-Marín, R.P.V. Faria, A.M. Ribeiro, et al. Biogas upgrading by selective adsorption onto CO_2 activated carbon from wood pellets, J. Environm. Chem. Engn. 5 (2017) 1386-1393.

[17] G.B. Wenz, W.J. Koros, Tuning carbon molecular sieves for natural gas separations: A diamine molecular approach, AIChE J. 63 (2017) 751-760.

[18] A.P. Terzyk, S. Furmaniak, R.P. Wesołowski, P.A. Gauden, P.J.F. Harris in Advances in Adsorption Technology, Editors: B. B. Saha and K.Ch. Ng, Nova Science Publishers Inc. 2010 pp.481-503.

[19] M.M. Dubinin, A.V. Astakhov, Theory of volume filling of micropores, Izv. AN SSSR Ser. Khim. 1 (1971) 5-24 (in Russian).

[20] K.A.G. Amankwah, J.A Schwarz, A modified approach for estimating pseudo-vapor pressures in the application of the Dubinin-Astakhov equation, Carbon 33 (1995) 1313-1319.

[21] S. Furmaniak, S. Koter, A.P. Terzyk, P.A. Gauden, P. Kowalczyk, G. Rychlicki, New insights into the ideal adsorbed solution theory, Phys. Chem. Chem. Phys. 17 (2015) 7232-7247.

[22] F.R. Siperstein, A.L. Myers, Mixed-gas adsorption, AIChE J. 47 (2001) 1141-1159.

[23] S.I. Sandler, Chemical and Engineering Thermodynamics, Wiley, New York 2010.

[24] W.H. Severns Jr., A. Sesonske, R.H. Perry, R.L. Pigford, Estimation of ternary vapour-liquid equilibrium, AIChE J. 1 (1955) 401-409.

[25] X. Zhou, W. Huang, J. Liu, H. Wang, Z. Li, Quenched breathing effect, enhanced CO_2 uptake and improved CO_2/CH_4 selectivity of MIL-53(Cr)/graphene oxide composites, Chem. Engn. Sci. 167 (2017) 98-104.

[26] P. Puthiaraj, Y.R. Lee, W.S. Ahn, Microporous amine-functionalized aromatic polymers and their carbonized products for CO_2 adsorption, Chem. Engn. J. 319 (2017) 65-74.

[27] C. Zhu, A porous Cd(II) metal-organic framework with high adsorption selectivity for CO_2 over CH_4, J. Molec. Struct. 1136 (2017) 140-143.

[28] S. Velioglu, M.G. Ahunbay, S.B. Tantekin-Ersolmaz, Novel co-polyimides containing pBAPS (bis [4-(4-aminophenoxy) phenyl] sulfone) for CO_2 separation, Sep. Purif. Technol. 178 (2017) 90-104.

[29] S.Y. Sawant, K.M. Rajesh, S. Somani, M. John, B.L. Newalkar, H.C. Bajaj, Precursor suitability and pilot scale production of super activated carbon for greenhouse gas adsorption and fuel gas storage, Chem. Engn. J. 315 (2017) 415-425.

[30] A.M. Saeed, P.M. Rewatkar, H.M. Far, T. Taghvaee, S. Donthula, C. Mandal et al. Selective CO_2 Sequestration with Monolithic Bimodal Micro/Macroporous Carbon Aerogels

Derived from Stepwise Pyrolytic Decomposition of Polyamide-Polyimide-Polyurea Random Copolymers, ACS Appl. Mater. Interf. 9 (2017) 13520-13536.

[31] J. Liu, G.P. Yang, Y. Wu, Y. Deng, Q. Tan, W.Y. Zhang et al. New luminescent three-dimensional Zn(II)/Cd(II)-based metal-organic frameworks showing high H_2 uptake and CO_2 selectivity capacity, Cryst. Growth Des. 17 (2017) 2059-2065.

[32] C. Wang, J. Liu, J. Yang, J. Li, A crystal seeds-assisted synthesis of microporous and mesoporous silicalite-1 and their $CO_2/N_2/CH_4/C_2H_6$ adsorption properties, Microp. Mesop. Mater. 242 (2017) 231-237.

[33] P. Billemont, N. Heymans, P. Normand, G. De Weireld, IAST predictions vs co-adsorption measurements for CO_2 capture and separation on MIL-100 (Fe), Adsorption 23 (2017) 225-237.

[34] D. Saha, G. Orkoulas, J. Chen, D.K. Hensley, Adsorptive separation of CO_2 in sulfur-doped nanoporous carbons: Selectivity and breakthrough simulation, Microp. Mesop. Mater. 241 (2017) 226-237.